Determination of the Spectral Properties and Harmonic Levels for Driving an Induction Motor by an Inverter Driver under the Different Load Conditions

S. Taskin, H. Gokozan

Turgutlu Vocational High School, Industrial Automation Department, Celal Bayar University,
Turgutlu, Manisa, Turkey, phone:+ 90 236 313 55 02; e-mail: sezai.taskin@ cbu.edu.tr

Introduction

The aim of the electric power system is to generate electrical energy and to deliver this energy to the end-user equipment at an acceptable voltage [1]. The quality of electricity has become a strategic case for electricity companies. With the increasing use of power electronics devices and nonlinear loads in electric power system, the issue of harmonics is becoming more and more importance [2].

Non-linear loads connected to AC electric networks generate undesired harmonics in the current dynamics which are usually responsible of additional power losses and the risk of equipment damage or malfunctioning [3]. The term harmonics can be defined as sinusoidal component of a periodic wave having a frequency that is an integral multiple of the fundamental frequency. If the fundamental frequency is 50 Hz, then the second harmonic is a sinusoidal wave of 100 Hz, the fifth harmonic is a sinusoidal wave of 250 Hz and so on. [4, 5]. Presence of these harmonics results in increased losses, equipment heating and loss-of-life, and interference with protection, control and communication circuits as well as customer loads [6].

In the industry, three-phase induction motors are seen as the most widely used machines. They are in a simple construction and have high reliability [7]. In the last few decades, the induction motors have evolved from being a constant speed motor to a variable speed, variable torque machine. With the invention of variable voltage, variable frequency drives, the use of an induction motors have increased [8]. However, these drives are important harmonic sources in the electric power systems.

Reference [8] presents harmonic analysis of motor current signatures under different fault conditions of medium and high power Variable Frequency Driver (VFD) systems. Also, reference [4] has investigated reviews the progress made in power system harmonics research and development since its inception. In the reference [9], a fuel pump induction motor in cement industries is investigated.

The Matlab/Simulink model for the sine pulse-width modulated (PWM) inverter results are discussed in steady state running mode and voltage/frequency (V/F) mode. Also the study [10] deals with the numerical modeling of a PWM voltage inverter-fed induction motor drive for the common and differential current modes. Another work has presented a probabilistic method to study the harmonic contents of voltage in direct torque controlled of induction motors [11].

Reference [12] shows a critical evaluation of the effect of various abnormal voltage conditions, balanced non-sinusoidal power supply, input voltage sags and short time blackout of power supply on matrix converter fed induction motor drives.

In this study, 3-phase currents of the motor are collected and analyzed using the spectral analysis methods like short-time Fourier transform and auto-power spectral density. Here, the short time Fourier transform is applied to overall current signal, which includes the all operational conditions, as an application of the non-stationary signal analysis. After the determination of the operational region in terms of the harmonic levels under the full-load condition, the auto-power spectral density is applied to this signal part, which can be accepted as a stationary signal approximately.

Harmonics and Power Quality

The most common indication of harmonics presence is Total Harmonic Distortion (THD) factor, which can be obtained both voltage and current as shown in Eq. [1, 2] [13]:

$$THD_{(V)} = \sqrt{\frac{\sum_{n=2}^{\infty} V_n^2}{V_1^2}}, \qquad (1)$$

$$THD_{(I)} = \sqrt{\frac{\sum_{n=2}^{\infty} I_n^2}{I_1^2}}, \qquad (2)$$

where V_1 and I_1 *are* the RMS values of the fundamental component of voltage and current, V_n and I_n are the RMS values of the nth harmonic component of voltage and current respectively.

Determining power quality components can be defined such as [14]:

- Continuity of electrical energy demand ;
- Frequency;
- Active voltage value;
- Transient voltage sags & swells;
- Rapid voltage changes;
- Unbalance among phase voltages;
- Harmonic components in voltage and current waveforms;
- Flicker.

It is an ideal situation that these components are continuously stable at the nominal value (frequency, voltage, etc...), or there is no component (sags and swells, rapid voltage changes, unbalance, flicker...), or the supply continuity is %100 (no electricity interruption). But, this is not valid for any electricity system. It has been defined in various national and international standards that to which extent the nominal value of most of the components can deviate. The more technology improves, it is expected that the less deviation will be permitted to occur depending on the nominal values [14].

Mathematical Methods

In this study, considered mathematical analysis tool is based upon the Fourier based techniques like power spectral density calculation as well as short-time Fourier transform approach.

Auto-power Spectral Density. A common approach for extracting the information about the frequency features of a random signal is to transform the signal to the frequency domain by computing the discrete Fourier transform. For a block of data of length N samples the transform at frequency $m\Delta f$ is given by (3)

$$X(m\Delta f) = \sum_{k=0}^{N-1} x(k\Delta t)\exp[-j2\pi km/N],\quad (3)$$

where Δf is the frequency resolution and Δt is the data-sampling interval. The auto-power spectral density (APSD) of $x(t)$ is estimated as

$$S_{xx}(f) = \frac{1}{N}|X(m\Delta f)|^2, \; f = m\Delta f. \quad (4)$$

The cross power spectral density (CPSD) between $x(t)$ and $y(t)$ is similarly estimated. The statistical accuracy of the estimate in (4) increases as the number of data points or the number of blocks of data increases [15].

Short-Time Fourier Transform. The short-time Fourier Transform (STFT), introduced by Gabor in 1946, and is useful in presenting the time localization of frequency components of signals [16]. The STFT spectrum is obtained by windowing the signal through a fixed dimension window. The signal may be considered approximately stationary in this window. The window dimension fixes both time and frequency resolutions. To

define the STFT, let us consider a signal x(t) with the assumption that it is stationary when it is windowed through a fixed dimension window g(t), centered at time location τ. The Fourier transform of the windowed signal yields the STFT [17]

$$STFT(\tau, f) = \int_{-\infty}^{+\infty} x(t)g(t-\tau)\exp[-j2\pi ft]dt. \quad (5)$$

Equation (5) maps the signal into a two-dimensional function in the time-frequency (t, f) plane. The analysis depends on the chosen window $g(t)$. Once the window $g(t)$ is chosen, the STFT resolution is fixed over the entire time-frequency plane.

Harmonics Measurement System based on LabVIEW and Experimental Set-up

Power quality measurement system is designed with LabVIEW^{TM} graphical program. The overall block diagram of the measurement system is shown in Fig. 1. The system consists of voltage and current transducers, connector block, data acquisition card and processing computer. National Instruments (NI) PCI 6221 multifunction data acquisition card, LEM HTR 500-SB current and LEM CV3-500 voltage transducers are used as measurement hardware. The DAQ card sampling rate is 250 *kS/s*. The power system has been supplied by 2500 *kVA* power transformator. Using this system, harmonic parameters of three-phase voltage and current signals, such as the THD and the distortions of the 1st to the 50th harmonics can be measured.

The input signals are connected into the data acquisition card for conversion to digital signals, which are afterwards collected, analyzed, computed, and output by the computer. Measurement results can be displayed as a real-time, printed and stored [18]. The power quality measurement system set-up is shown in Fig. 1.
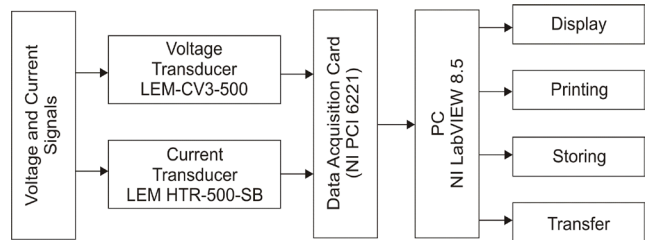

Fig. 1. Block diagram of the power quality measurement system

Fig. 2 shows the LabVIEW's visual front panel for the power quality measurement system. Data recording sampling rate is selected as 5000 S/s. While conducting the power quality measurements, related standards which are IEEE-519-1992, EN 50160, IEC 61000-4-7 and IEC 61000-4-30, are considered.

Application of the Data and Results

There are two aspects of the application in terms of the collected data. These are non-stationary data in which motor gets the different load condition step by step and stationary data for full load condition.
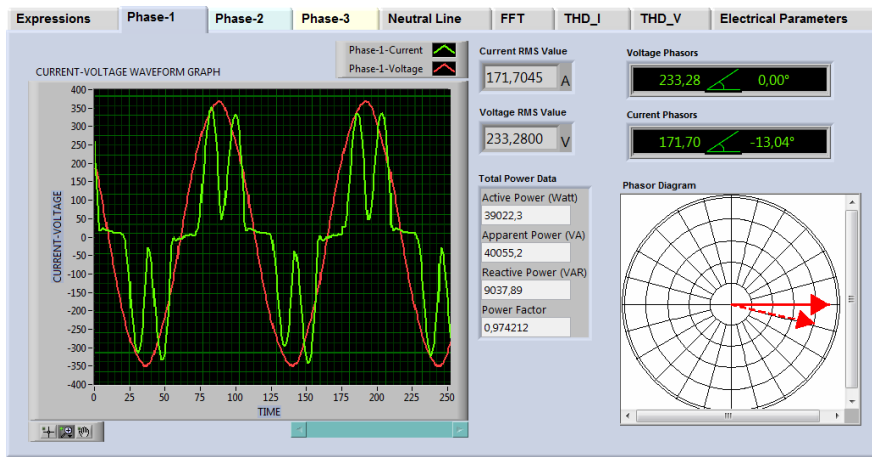
Fig. 2. User-interface of the measurement system based on LabVIEW[TM]

Non-stationary case under the different load condition. In this application, 75 *kW* induction motor is fed through power transformator group of 2500 *kVA*. For this reason voltage variations reflect the properties of a balanced system as indicated by Fig. 3. Phase current variations are also presented as shown in Fig. 4. As seen from this figure, there are four different operation regions like no-load condition between 0 – 7.14 seconds; transient case between 7.14 – 8 seconds, transition to full load between 8 – 9.5 seconds and the full load condition between 9.5 – 13 seconds respectively. For more detailed consideration, spectral study is applied on the one phase variation of the currents.

Under the assumption of the similar properties of the current signals, the phase-1 is considered for the spectral analysis and its spectrogram is given by Fig. 5.
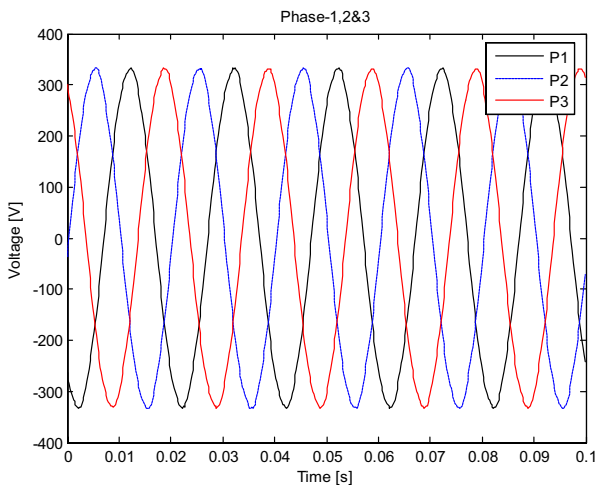

Fig. 3. Voltage variations for three phases (P1, P2 and P3)

As seen in the Fig. 5 the most dominant harmonics appear under the full load condition between the 9.5 and 12 seconds. Here the effective harmonics are 3, 5, 7, 11, 13, 17 and 19th. However, in the transient region fundamental frequency at 50 *Hz* occurs and after two seconds, the other harmonics like 5 and 7th harmonics appear. The full-load region can be accepted as almost stationary region. In order to get more detailed information about the harmonics, Fig. 5 is restricted between 0 and 1000 *Hz* in

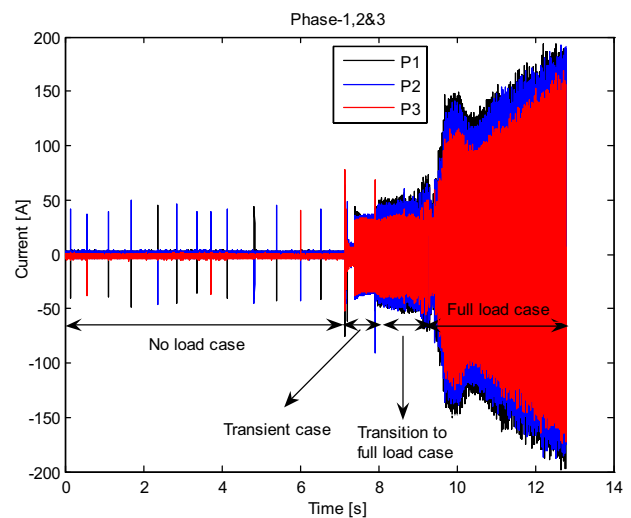terms of the frequency axis and then it can be shown by Fig. 6.

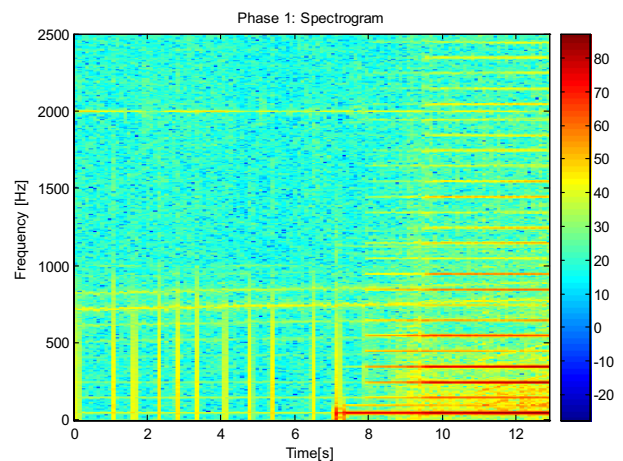**Fig. 4.** Supply current variations by the inverter of the motor

Fig. 5. Spectrogram of the phase-1

As seen from the Fig. 6, dominant frequencies are 3, 5, 7, 11, 13, 17 and 19th harmonics as well as the fundamental frequency at 50 *Hz*. In addition to these, the second harmonic at 100 *Hz* is also observed with a minor effect at the beginning of the transient region. Also, measurement noise appears at around 720 *Hz* for overall time. However,

bad data effects like noise are observed by the perpendicular lines before the transient case.
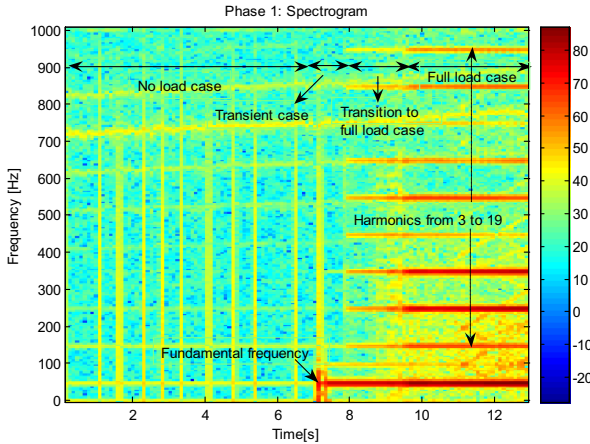

Fig. 6. Spectrogram of the phase-1 for zoomed case

Stationary case for full load condition. Under this section, motor current variations, which are defined both of the time and frequency domain, are considered. For this purpose, three current variations at full load are shown within very short time as given in Fig. 7.
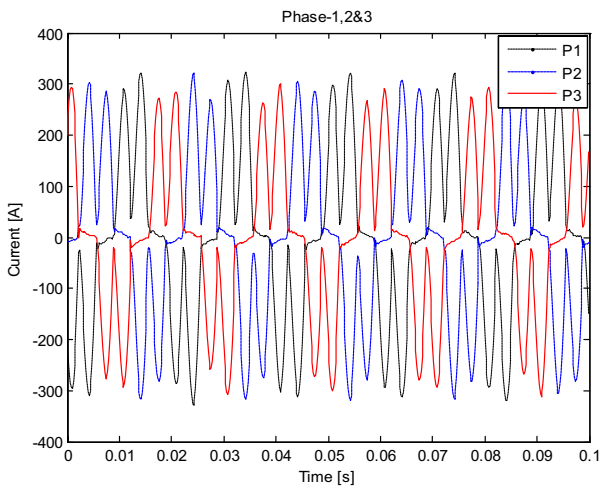

Fig. 7. Induction Machine current variations at full load condition

In order to find the frequency contest of the one of the phase currents, Power Spectral Density approach is applied to the phase-1 and its result can be seen in Fig. 8. below. Here dominant frequency components are odd harmonics from 3rd to 19th harmonics as well as the fundamental frequency at 50 *Hz*. And also, it can be said that all odd harmonic components change from 3rd to 49th.

Here, it can be considered a threshold to define more meaningful harmonics. This threshold is determined considering the full load region, which is defined between the 9.5 and 12 seconds, in the Fig. 6. In this time-frequency plane, maximum harmonic level is at 850 *Hz* as 17th harmonic component. For this reason, the threshold level is selected at logarithmic current value of 10^4 and then it can be shown by Fig. 9.
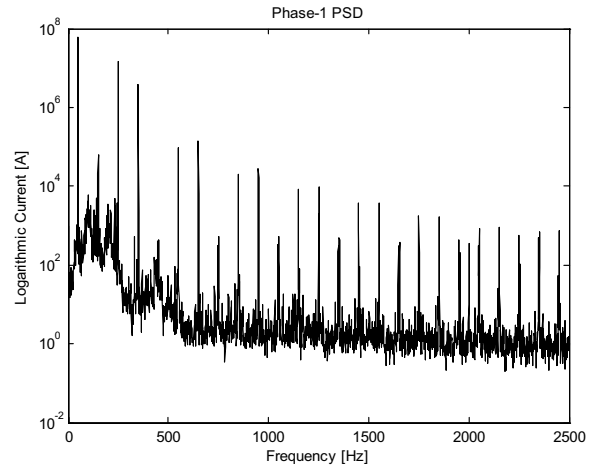

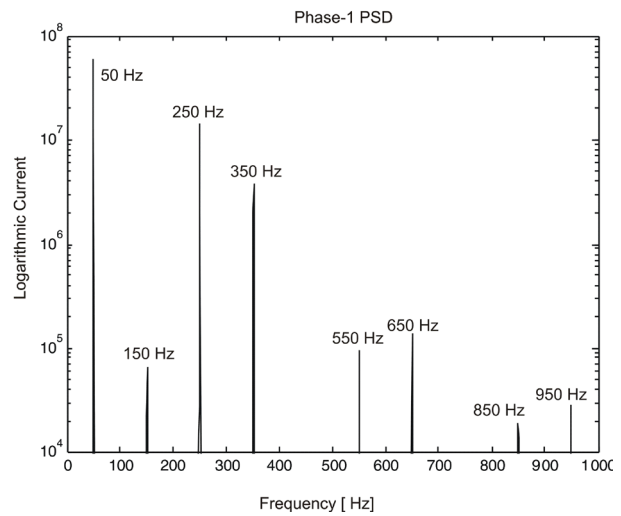**Fig. 8.** PSD of motor current variations for phase 1 at full load condition

Fig. 9. Zoomed PSD for phase-1 regarding to selected threshold value

As seen in Fig. 9, dominant harmonic frequencies take place at 150, 250, 350, 550, 650, 850 and 950 *Hz*. These are respectively 3rd, 5th, 7th, 11th, 13th, 17th and 19th harmonics. Hence, it is seen that these harmonics are extremely consistent with the results of the non-stationary case as shown in the Fig. 6.

Also, some important harmonic levels regarding to the fundamental component can be shown by the Table 1.

Table 1. Calculated harmonic ratios

Harmonics	Harmonic Ratios (%)
50 Hz, Fundamental frequency	100
150 Hz, 3rd Harmonic	0,11
250 Hz, 5th Harmonic	24
350 Hz, 7th Harmonic	6.3
550 Hz, 11th Harmonic	0.16
650 Hz, 13th Harmonic	0.23
850 Hz, 17th Harmonic	0.032
950 Hz, 19th Harmonic	0.047

As seen in the Table 1, the most dominant harmonic ratio is 5th harmonic. Also, 7th harmonic is second important harmonic level. In this manner, both of the 5th

and 7th harmonics exceed the critical value of the total harmonic distortion (THD) level, this critical value is notified around 5% of the THD for current in harmonic standard of IEEE, which is indicated as IEEE-519-1992 in the reference list. For this reason, these harmonics must be filtered using an appropriate filter structure.

Conclusions

In this study, harmonic levels and some distortion ratios were considered for the current measurement of an induction motor, which is driven by an inverter. For this purpose, there are two stages of this experimental study. The first one is under the load changes gradually and the second one is related to the full load condition. Under these experimental results, some of the findings can be listed as below.

1. For the non-stationary data, current signal can be represented by four regions like no-load region; transient case; transition to full load and the full-load condition:
   ♦ These operational regions are used to determine the harmonic levels.
   ♦ For no-load region, harmonic level has never been.
   ♦ For the transient case, dominant frequency is fundamental frequency of 50 *Hz*.
   ♦ For the transition region to full load region, all odd harmonics are given from 3rd to 13th harmonic, excepting 9th harmonic, as well as fundamental frequency.
   ♦ For the full load region, all odd harmonics are given from 3rd to 19th harmonics excepting the 9th and 15th harmonics.
2. For the stationary region (it means the measurements for full load condition); harmonic frequencies take place at 150, 250, 350, 550, 650, 850 and 950 *Hz* regarding a selected threshold. These are respectively 3rd, 5th, 7th, 11th, 13th, 17th and 19th harmonics. Hence, it is seen that these harmonics are extremely consistent with the results of the non-stationary case as above.

Consequently, these harmonic levels are considered as effect of the inverter used in this study. For the full-load condition the total harmonic distortion (THD) is calculated as 24% of the fundamental component.

References

1. **Xu, L., , Han, Y., Pan, J., Chen, C.,, Yao, G.,, Zhou, L.D** . Selective Compensation Strategies for the 3-phase Cascaded Multilevel Active Power Filter using ANF-based Sequence Decoupling Scheme // Electronics and Electrical Engineering. – Kaunas: Technologija, 2010. – No. 2(98). – P. 15–20.

2. **Bukšnaitis J.** Power Indexes of Induction Motors and Electromagnetic Efficiency their Windings // Electronics and Electrical Engineering. – Kaunas: Technologija, 2010. – No. 4(100). – P. 11–14.
3. **Marconi L., Ronchi F., Tilli A.** Robust Nonlinear Control of Shunt Active Filters for Harmonic Current Compensation // Automatica, 2007. – Vol. 43. – P. 252–263.
4. **Singh G. K.** Power System Harmonics Research: A Survey // European Transactions on Electrical Power, 2009. – Vol. 19. – P.151–172.
5. **Deltuva R., Virbalis, J. A. Gečys S.** Electric and Magnetic Fields of the High Voltage Autotransformer // Electronics and Electrical Engineering. – Kaunas: Technologija, 2010. – No. 10(106). – P. 9–12.
6. **Pandian G., Reddy S. R.** Simulation and Analysis of Multilevel Inverter Fed Induction Motor Drive // Indian Journal of Science and Technology, 2009. – Vol. 2. – P. 67–69.
7. **Vicente P., Rodriguez J., Negrea M., Arkkio A.** A Simplified Scheme for Induction Motor Condition Monitoring // Mechanical Systems and Signal Processing, 2008. – Vol. 22. – P.1216–1236.
8. **Biswas B., Das S., Purkait P., Mandal M.S., Mitra D.** Current Harmonics Analysis of Inverter–Fed Induction Motor Drive System under Fault Conditions // Proceedings of the International MultiConference of Engineers and Computer Scientists (IMECS'2009), 2009. – Vol II.
9. **Sasikumar M., Pandian S.C.** Performance and Harmonic Analysis of PWM Inverter–fed Induction Motor Drives System // International Journal on Electronic and Electrical Engineering, 2009. – Vol. 6. – No. 9. – P. 41–46.
10. **Bartos S., Dolezel I., Necesany J., Skramlik J., Valouch V.** Electromagnetic Interferences in Inverter–Fed Induction Motor Drives // International Conference on Renewable Energies and Power Quality, 2008.
11. **Kaboli S., Vahdati E., Zolghadri M. R.,** Probabilistic Voltage Harmonic Analysis of Direct Torque Controlled Induction Motor Drives // IEEE Transactions on Power Electronics, 2006. – Vol. 21. – No. 4. – P. 1041–1052.
12. **Kumar V., Bansal R. C., Joshi R. R.** Drive under Various Abnormal Voltage Conditions // International Journal of Control, Automation, and Systems, 2008. – Vol. 6. – No. 5. – P. 670–676.
13. **Ferracci P.** Power Quality // Cahier Technique Schneider Electric, 2001. – No. 199.
14. Turkey National Power Quality Project Document, What is power quality?, 2010. Online: http://www.guckalitesi.gen.tr/en/.
15. **Seker S., Ayaz E.** A Reliability Model for Induction Motor Ball Bearing Degradation // Electric Power Components and Systems, 2003. – Vol. 31. – No. 7. – P. 639–652.
16. **Taskin S., Seker S., Karahan M., Akinci C.** Spectral Analysis for Current and Temperature Measurements in Power Cables // Electric Power Components & Systems, 2009. – Vol. 37. – No. 4. – P. 415–426.
17. **Seker S.,** Determination of Air–gap Eccentricity in Electric Motors Using Coherence Analysis // IEEE Power Engineering Review, 2000. – Vol. 20. – No. 7. – P. 48–50.
18. **Tang G., Wang Y., Guo S.,** Design of Power System Harmonic Measurement System Based on LabVIEW // Proc. of fourth International Conference on Natural Computation, 2008. – P. 489–493.

S. Taskin, H. Gokozan. Determination of the Spectral Properties and Harmonic Levels for Driving an Induction Motor by an Inverter Driver under the Different Load Conditions // Electronics and Electrical Engineering. – Kaunas: Technologija, 2011. – No. 2(108). – P. 75–80.

This paper analyses the electrical power quality for the induction motor of 75 *kW* using the spectral analysis methods. Measurements are carried out by collecting the current and voltage variations in a ceramic factory. Spectral analyzing techniques are applied to the collected data to get the spectral properties. Hence, induction motor operation regions are categorized under three zones. These are no-load condition; transient case from no-load to load and full-load, respectively. Consequently, the variations of the harmonics are compared with each other under these different operation conditions and then the most important characteristics of the harmonics are determined. In this manner, dominant harmonics are obtained as 5th, 7th, 11th, 13th and 17th harmonics as well as fundamental frequency at 50 *Hz*. Ill. 9, bibl. 18, tabl. 1 (in English; abstracts in English and Lithuanian).

S. Taskin, H. Gokozan. Valdomų asinchroninių variklių spektrinių savybių ir harmonikų lygių nustatymas esant įvairioms apkrovos sąlygoms // Elektronika ir elektrotechnika. – Kaunas: Technologija, 2011. – Nr. 2(108). – P. 75–80.

Taikant spektrinės analizės metodus analizuojama asinchroninio 75 kW galios variklio elektros energijos kokybė. Išmatuotos įvairios srovės ir įtampos kombinacijos. Surinktiems duomenims pritaikytas spektrinės analizės metodas. Tokio variklio darbo režimai skirstomi į tris grupes: tuščioji eiga, įsibėgėjimas, visa apkrova. Palygintos įvairių kombinacijų harmonikos ir nustatytos pačios svarbiausios. Nustatyta, kad dominuojančios harmonikos, esant 50 Hz dažnui, yra penktoji, septintoji, vienuoliktoji, tryliktoji ir septynioliktoji. Il. 9, bibl. 18, lent. 1 (anglų kalba; santraukos anglų ir lietuvių k.).